5.2 Artifacts in the EEG

One of the most important issues in computer-based biomedical signal processing is noise/artifact cancellation/reduction when the signal is corrupted with additive and multiplicative noise or in cases where the desired information constitutes only a part of the signal such that irrelevant portions are considered as artifact. Based on their origin, EEG artifacts are divided into two physiological and technical classes which are known as artifact and noise, respectively. While the influence of technical noise can be highly reduced by improving the electrode design and attachment techniques, the corruptive effect of artifacts of physiological origin is inevitable. Accordingly, a vast majority of EEG artifact cancellation/reduction algorithms are developed to reduce the physiological artifacts caused by electrical activity of other electrophysiological sources such as cardiac activity, muscle movement, eye movement and blinks. Depend on the task and recording situation, multiple types of artifacts may be presented at the same time.

5.2.1 Common EEG Artifacts

The most common types of EEG artifacts are:

- **Eye movement and blinks:**
  The electrical potential difference between the cornea and the retina changes during the eye movement and produces Electrooculogram (EOG) signal. Depend on the proximity of the EEG electrode to the eye, the direction in which the eye is moving (i.e., horizontal or vertical eye movement) and the repetition pattern of eye movement, the strength of the interfering EOG signal is different. This artifact is present in EEG signals recorded both in awaking state and the REM phase of the sleep. Figure 5-5(a) depicts example of waveforms produced by repeated eye movement where the artifact can be distinguished from EEG pattern due to its repetitive character. However, in some cases, the EOG artifact can be confused with slow EEG activity such as theta and delta rhythms. Apart from eye movement, eyelid movement (‘blink’) also affects the corneal-retinal potential difference, hence, causes EEG artifact. Different from eye movement artifact, eyelid movement produces a more abruptly changing waveform, hence, high-frequency components are dominant in this artifact. Figure 5-5(b) shows a waveform produced by repetitive blinking which resembles a square wave. From Figure 5-5, it can be seen that the amplitude of

blinking artifacts in the frontal electrodes is substantially larger than that of the background EEG.

As later we see, in EEG signal processing, it is practically useful if a pure EOG signal can be recorded by means of two reference electrodes positioned near the eye which do not contain any EEG activity.

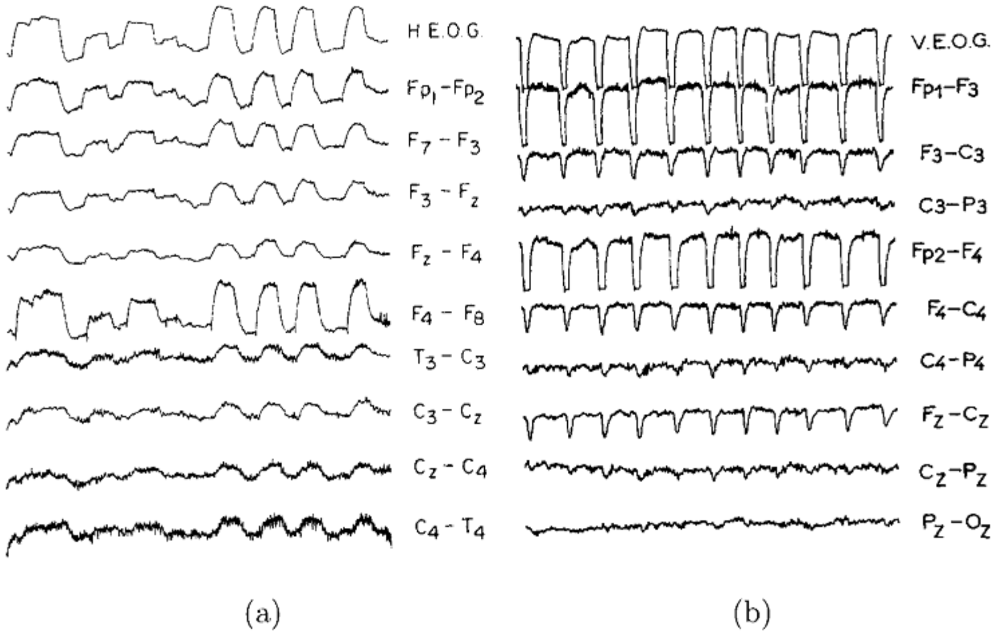

Figure 5-5: Artifacts in the EEG caused by a) eye movement and b) repetitive eyelid movement (voluntary blinking) [2].

- **Muscle activity:**

  The electrical activity of contracting muscles appears as another type of EEG artifact and can be measured on the body surface by the EMG. This artifact may occur due to swallowing, chewing, grimacing, frowning, talking, and hiccupping both in awake state and during sleep. However, the muscle artifact is considerably reduced during relaxation and sleep. The pattern of the EMG recordings is determined by the degree of muscle contraction; while a train of low amplitude rarely happening spikes is produced by a weak contraction, more frequent spikes with less inter-spike intervals are recorded in stronger contraction such that the overall shape of EMG exhibits a continuously varying signal (see Figure 5-6).

From the artifact processing point of view, there exist two crucial bottlenecks in EMG artifact cancellation: i) the spectral properties of EMG considerably overlap with beta activity observed in EEG (in the $15 - 30\,Hz$ range), ii) it is impossible to acquire a reference signal containing only EMG activity.

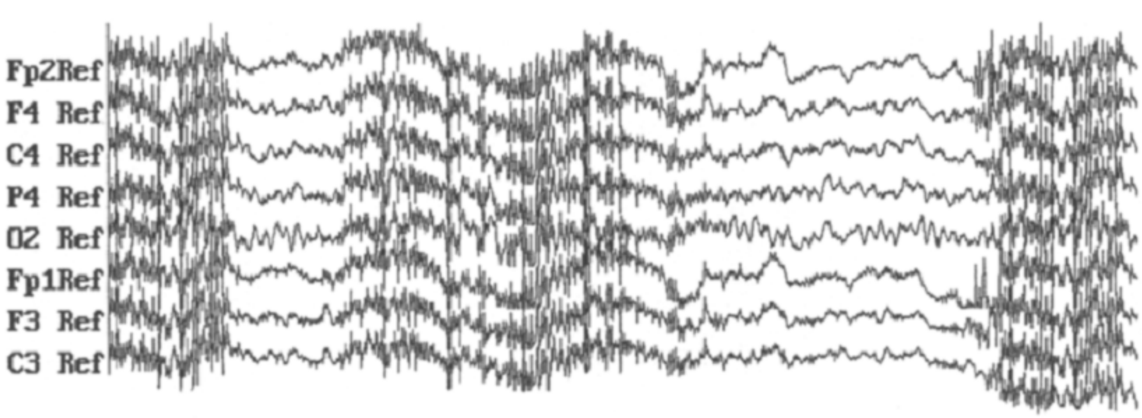

Figure 5-6: A 5-seconds multi-channel EEG recording contaminated by intermittent episodes of EMG artifact [2].

- **Cardiac activity**

  Depend on the electrode positions and the body shapes, the electrical activity of the heart (reflected in ECG) may interfere with the EEG. Since the normal heartbeats are characterized by repetitive, regularly occurring waveform pattern in ECG, it is easy to reveal if this artifact is present in EEG signal. However, in EEG signals with epileptic-form activity, presence of spike-shaped ECG waveforms might be misleading. This situation is exacerbated during the presence of certain cardiac arrhythmias in which ECG exhibits considerable variability in the interbeat interval.

  Similar to the EOG artifacts, the ECG can be acquired independently by one or several electrodes for use in canceling the ECG activity that may be superimposed on the EEG.

- **Electrodes and equipment:**

  Similar to any other biomedical measurement on the body surface, movement of EEG recording electrodes produces an artifact commonly referred to as the “electrode-pop” artifact. Indeed, this movement changes the DC contact potential at the electrode-skin interface and causes to observe an abrupt change in the baseline level of EEG signal, followed by a slow, gradual return to the original baseline level. Therefore, this artifact can be deceptive in spike or sharp epileptic wave detection.

Another possible source of artifact is the electrode wire which connects the electrode to the acquisition equipment. If the electrode is not properly shielded, the electromagnetic field produced by currents flowing in nearby powerlines or electrical devices may cause a strong $50/60\ Hz$ powerline interference. Finally, equipment-related artifacts include those produced by internal amplifier noise and amplitude clipping caused by an analog-to-digital converter with too narrow dynamic range.

5.2.2 Artifact Processing

The scope of artifact processing ranges from a simple *artifact rejection* to complete *cancellation of the artifact* from the EEG signal. In artifact rejection, the objective is to create a simple marker to identify a specific artifact and exclude the segments of poor quality (i.e., those contaminated by the artifact) from further processing. It is of particular importance in handling those segments of EEG which contain excessive EMG interference, specially, when the dataset consists of short time recordings. On the other side, artifact cancellation is a preprocessing stage which conditions the EEG signal for better visual reading and interpretation or subsequent analysis. In either case, it is essential that the development of algorithms for artifact cancellation is accompanied by visual assessment to assure that the performance is acceptable.

Artifact processing algorithms commonly include two successive steps: i) noise/artifact estimation from a signal measured on the scalp or from available reference signals (e.g., EOG to remove eye movement artifact) and ii) (estimated) noise/artifact subtraction from the observed signal, $x[n]$. In this approach, it is assumed that $x[n]$ is sum of cerebral activity, $s[n]$, and noise, $v[n]$, i.e.:

$$x[n] = s[n] + v[n]. \tag{5-34}$$

There exist another type of model in which the signal and noise interact in a multiplicative way such that:

$$x[n] = s[n]v[n]. \tag{5-35}$$

Additive model, explained by Eq. (5-34), received a great popularity due to its simplicity and existing methods for optimal estimation of $s[n]$. Techniques for separating multiplicative noise from $s[n]$, however, have only received marginal attention in the area of EEG signal processing.

5.2.3 Artifact Reduction Using Linear Filtering

In many EEG processing algorithms, linear, time-invariant filtering is considered for the reduction of $50/60\ Hz$ power-line interference and EMG artifacts. In this technique, a LTI filter is designed to shape the frequency spectrum of the observed signal by suppressing particular frequency components. Low-pass filtering is an example which is used to remove power line noise and to reduce the influence of EMG activity when the analysis of slower EEG rhythms is of interest. Unfortunately, applicability of such filters is limited because the spectra of the EEG and the artifacts overlap each other considerably. Besides, poorly designed LTI filters may either suppress relevant information (e.g., abrupt spike-shape wave forms if we use low-pass filters) or introduce spurious activity, resembling the beta rhythm.

In addition to LTI filters, various nonlinear filter structures have been suggested to overcome these performance limitations, but such filters have not come into widespread use. In particular, the effects of poorly designed filters are highlighted for filters with nonlinear phase characteristics, since different frequency components will be delayed differently.

Linear filters are more practical for cancellation of powerline interference in ECG signals which will be briefly discussed in chapter 7.

5.2.4 Artifact Cancellation Using Linearly Combined Reference Signals

Since the artifacts caused by eye movement and blinks are very common, most artifact cancellation algorithms are developed to reduce the effect of these artifacts. In this section, the most popular approach is described in which an estimate of the EOG artifact is first computed and then subtracted from the EEG signal measured on the scalp. In order to estimate the EOG artifact, EOG signal is separately recorded by placing the electrodes around the eye so that horizontal and vertical movements are well-captured (see Figure 5-7).

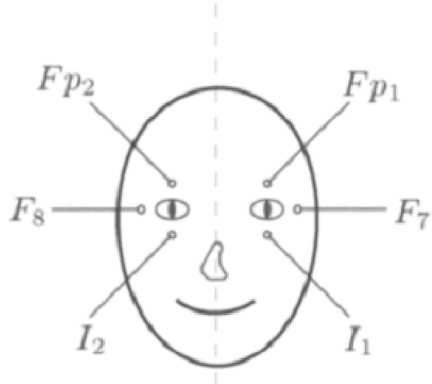

Figure 5-7: Electrode positions for recording EOG signals which reflects horizontal ($F_7 - F_8$) and vertical eye movement ($Fp_1 - I_1$ or $Fp_2 - I_2$) [2].

As it was mentioned above, in this approach, the EEG signal is supposed to be sum of cerebral activity, $s[n]$ and the EOG artifact, $v_0[n]$:

$$x[n] = s[n] + v_0[n]. \tag{5-36}$$

It is also assumed that the EOG reference signals, (i.e., $v_1[n], \dots, v_M[n]$) are linearly transferred into the EEG signal such that an artifact-cancelled signal, $\hat{s}[n]$ is estimated by subtracting a linear combination of the weighted reference signals from the EEG, using the weights, $w_1, \dots, w_M$:

$$\hat{s}[n] = x[n] - \sum_{i=1}^{M} w_i v_i[n] = s[n] + (v_0[n] - \boldsymbol{w}^{\boldsymbol{T}} \boldsymbol{v}[n]), \tag{5-37}$$

where $\boldsymbol{v}[n] = (v_1[n], \dots, v_M[n])^T$ and $\boldsymbol{w}[n] = (w_1[n], \dots, w_M[n])^T$. Therefore, the estimate of the EOG artifact is obtained by $\hat{v}_0[n] = \boldsymbol{w}^{\boldsymbol{T}} \boldsymbol{v}[n]$. The third assumption is that all signals are random with zero-mean, and that $s[n]$ is uncorrelated with the EOG signals $\boldsymbol{v}[n]$ at each time n, such that:

$$\mathcal{E}\{s[n] v_i[n]\} = 0, i = 1, \dots, M. \tag{5-38}$$

The block diagram in Figure 5-8 summarizes the method.

In order to estimate the EOG artifact (i.e., $\hat{v}_0[n] = \boldsymbol{w}^{\boldsymbol{T}} \boldsymbol{v}[n]$), the values of different weights need to be determined. One way is to minimize the mean-square error (MSE), $E_{\boldsymbol{w}}$ between $x[n]$ and the linearly combined reference signals with respect to $\boldsymbol{w}$,

$$E_{\boldsymbol{w}} = \mathcal{E}\{(x[n] - \boldsymbol{w}^{\boldsymbol{T}} \boldsymbol{v}[n])^2\}. \tag{5-39}$$

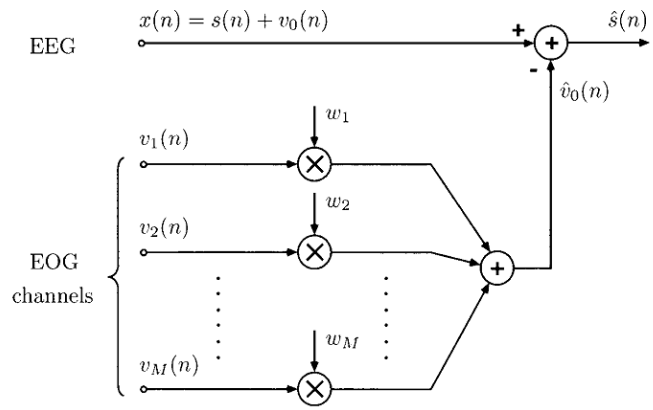

Figure 5-8: Cancellation of eye movement artifact based on linear combination of EOG signals using the fixed weights [2].

Since $s[n]$ is assumed to be uncorrelated with the EOG artifacts, $v_i[n]$, the MSE, $E_{\boldsymbol{w}}$, can alternatively be expressed as

$$E_{\boldsymbol{w}} = \mathcal{E}\{s^2[n]\} + \mathcal{E}\{(v_0[n] - \boldsymbol{w}^{\boldsymbol{T}}\boldsymbol{v}[n])^2\}, \tag{5-40}$$

which implies that the dropping the offset, $\mathcal{E}\{s^2[n]\}$, weights $\boldsymbol{w}$ should be chosen such that the error between $v_0[n]$ and $\boldsymbol{w}^{\boldsymbol{T}}\boldsymbol{v}[n]$ is minimized. Differentiation of $E_{\boldsymbol{w}}$ in Eq. (5-39) with respect to the coefficient vector $\boldsymbol{w}$ yields:

$$\frac{\partial E_{\boldsymbol{w}}}{\partial \boldsymbol{w}} = \frac{\partial(\mathcal{E}\{x^2[n]\} + \boldsymbol{w}^{\boldsymbol{T}}\boldsymbol{R}_{\boldsymbol{v}}[n]\boldsymbol{w} - 2\boldsymbol{w}^{\boldsymbol{T}}\varphi_{xv}[n])}{\partial \boldsymbol{w}} = 2\boldsymbol{R}_{\boldsymbol{v}}[n]\boldsymbol{w} - \boldsymbol{2}\varphi_{xv}[n]. \tag{5-41}$$

The correlation matrix $\boldsymbol{R}_{\boldsymbol{v}}[n]$ of the reference signals describes the spatial correlation between the different channels at each time n and is defined by:

$$\boldsymbol{R}_v[n] = \mathcal{E}\{\boldsymbol{v}[n]\boldsymbol{v}^T[n]\} = \begin{bmatrix} \varphi_{v_1v_1}[n] & \varphi_{v_1v_2}[n] & \dots & \varphi_{v_1v_M}[n] \\ \varphi_{v_2v_1}[n] & \varphi_{v_2v_2}[n] & \dots & \varphi_{v_2v_M}[n] \\ \vdots & \vdots & \ddots & \vdots \\ \varphi_{v_Mv_1}[n] & \varphi_{v_Mv_2}[n] & \dots & \varphi_{v_Mv_M}[n] \end{bmatrix}. \tag{5-42}$$

where

$$\varphi_{v_iv_j}[n] = \mathcal{E}\{v_i[n]v_j[n]\}\,. \tag{5-43}$$

The cross-correlation vector $\varphi_{xv}[n]$ between $x[n]$ and $\boldsymbol{v}[n]$ is defined by:

$$\varphi_{xv}[n] = \mathcal{E}\{x[n]\boldsymbol{v}[n]\} = (\varphi_{xv_1}[n], \varphi_{xv_2}[n], \dots, \varphi_{xv_M}[n])^T\,, \tag{5-44}$$

where

$$\varphi_{xv_i}[n] = \mathcal{E}\{x[n]v_i[n]\}\,. \tag{5-45}$$

In reality, the correlation quantities $\boldsymbol{R}_v[n]$ and $\varphi_{xv}\ [n]$ are time varying, but for simplicity, for now we assume that these quantities are time-invariant over the observation interval (i.e., $\boldsymbol{R}_v[n] \equiv \boldsymbol{R}_v$ and $\varphi_{xv}\ [n] \equiv \varphi_{xv}$ for $n = 1, \dots, N-1$).

Setting the gradient in Eq. (5-41) equal to zero, the following system of linear equations are obtained:

$$\boldsymbol{R}_v \boldsymbol{w} = \varphi_{xv} \tag{5-46}$$

whose solution yields the optimal weight vector $\boldsymbol{w}^*$. Then, the corresponding minimum MSE is easily found by insertion of Eq. (5-45) in Eq. (5-39),

$$E_{\boldsymbol{min}} = \mathcal{E}\{x^2[n]\} - (\boldsymbol{w}^*)^{\boldsymbol{T}} \boldsymbol{R}_v \boldsymbol{w}^*. \tag{5-47}$$

In practice, the spatial correlations $\varphi_{v_i v_j}$ need to be estimated from the measured EOG signals prior to computation of $\boldsymbol{w}$. Since $\boldsymbol{R}_v$ is considered to be fixed in time, it is estimated by simply replacing $\mathcal{E}\{v_i[n]v_j[n]\}$ by the corresponding time average,

$$\hat{\varphi}_{v_i v_j} = \frac{1}{N} \sum_{n=0}^{N-1} v_i[n] v_j[n]. \tag{5-48}$$

The cross-correlation vector φ_{xv} can be estimated in the same way. The procedure to find the values of the optimal weight vector $\boldsymbol{w}^*$ is then repeated for each of the available EEG channels in order to produce channel-specific weights. Figure 5-9 shows the performance of the EOG cancellation method, where artifact cancellation is based on two reference signals, i.e., $M = 2$.

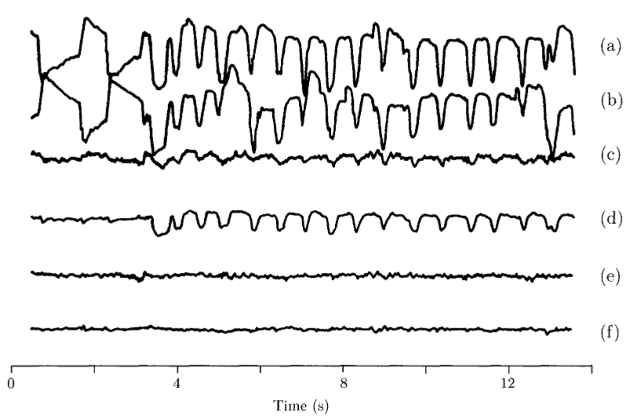

Figure 5-9: An example of EOG artifact cancellation in EEG signals. a,b) EOG signals measured for right and left eyes. c,d) EEG signals from two different electrodes before and e,f) after artifact cancellation [2].

Table 5-1 summarizes the algorithm.

Table 5-1: An algorithm for artifact cancellation using linearly combined reference signals

Inputs:
- $\boldsymbol{x_i[n], i = 1, \dots, P}$: **$\boldsymbol{P}$- Channel EEG recordings for $\boldsymbol{N}$ time sample (i.e., $\boldsymbol{n = 0, \dots, N-1}$)**
- $\boldsymbol{v_i[n], i = 1, \dots, M}$: **$\boldsymbol{M}$-Channel EOG for $\boldsymbol{N}$ time sample (i.e., $\boldsymbol{n = 0, \dots, N-1}$)**
Output:
- $\hat{s}[\boldsymbol{n}]$: **artifact-cancelled signal for $\boldsymbol{N}$ time sample (i.e., $\boldsymbol{n = 0, \dots, N-1}$)**
Procedure:
for $\boldsymbol{k = 1{:}P}$ do
for $\boldsymbol{i = 1{:}M}$ and $\boldsymbol{j = 1{:}M}$ do
- **estimate $\hat{\varphi}_{v_i v_j}$ using Eq. (5-48)**
- **estimate $\hat{\varphi}_{\boldsymbol{x_k} v}$ using Eq. (5-48) by replacing v_i with $\boldsymbol{x_k}$.**
- **create $\boldsymbol{R_v}$ using Eq. (5-42)**
- **solve Eq. (5-46), a linear regression problem to find $\boldsymbol{w}^*$**
- **calculate $\hat{s}_{\boldsymbol{k}}[n] = x_{\boldsymbol{k}}[n] - \sum_{i=1}^{M} \boldsymbol{w}_{\boldsymbol{i}}^* v_i[n]$**
end for
end for

It is worth mentioning that cancellation of ECG artifacts in the EEG can be performed in a similar way.

5.2.5 Adaptive Artifact Cancellation Using Linearly Combined Reference Signals

In the previous algorithm for EOG cancellation, the set of linear weights were fixed. Therefore, the algorithm is unable to track slow changes in EOG and its influence on EEG signal. In this section, a modified version of previous algorithm (known as Least Mean Square (LMS)) will be presented which has been developed to address this issue. Although this algorithm is the most commonly used in EEG processing, it is only one of many adaptive filtering algorithms developed for noise cancellation. Interested readers are referred to this paper for a review on various adaptive algorithms.

In this algorithm, $\boldsymbol{w}^T \boldsymbol{v}[n]$, in EOG artifact estimation, is replaced by $\boldsymbol{w}^T[n]\boldsymbol{v}[n]$ where the weight vector, $\boldsymbol{w}[\boldsymbol{n}]$ is a function of time. As a result, the mean-square error criterion becomes:

$$E_{\boldsymbol{w}}[n] = \mathcal{E}\{(x[n] - \boldsymbol{w}^{\boldsymbol{T}}[\boldsymbol{n}]\boldsymbol{v}[n])^2\} \tag{5-49}$$

which should be minimized with respect to $\boldsymbol{w}[\boldsymbol{n}]$. Since this objective function is quadratic, it has a unique minimum. Figure 5-10 depicts the $E_{\boldsymbol{w}}[n]$ when $\boldsymbol{w}[\boldsymbol{n}] = (w_1[n], w_2[n])^{\boldsymbol{T}}$is a two-dimensional vector. Because of time-varying nature of $\boldsymbol{v}[n]$, the optimal solution of $E_{\boldsymbol{w}}[n]$ changes with time, n. The method of *steepest descent* is, therefore, commonly used to find the minimum of this time varying nonlinear function. In this method, the current weight estimate, $\boldsymbol{w}[n]$ is updated by an adaptive correction term which pushes the next estimate $\boldsymbol{w}[n+1]$ towards the desired solution. The correction of $\boldsymbol{w}[n]$ is achieved by taking a step in the direction of the steepest descent of the quadratic error surface. This direction is given by the negative error gradient vector, i.e., the vector of partial derivatives of $E_{\boldsymbol{w}}[n]$ with respect to the weights $w_i[n]$ such that the $\boldsymbol{w}[n]$ is updated by the following equation:

$$\boldsymbol{w}[n+1] = \boldsymbol{w}[n] - \frac{1}{2}\mu \frac{\partial E_{\boldsymbol{w}}[n]}{\partial \boldsymbol{w}} \tag{5-50}$$

where the step size μ is a positive-valued scalar which determines the speed of adaptation. While small values of μ guarantee a less noisy estimate of $\boldsymbol{w}[n]$, it takes more time till the algorithm approaches the optimum solution. With large values of step size, the algorithm converges fast, but at the expense of a noisier estimate of $\boldsymbol{w}[n]$. Calculating the gradient vector of the error $E_{\boldsymbol{w}}[n]$ with respect to $\boldsymbol{w}$, we get:

$$\frac{\partial E_{\boldsymbol{w}}[n]}{\partial \boldsymbol{w}} = -2\mathcal{E}\{e[n]\boldsymbol{v}[n]\}, \tag{5-51}$$

where the error $e[n]$ is

$$e[n] = x[n] - \boldsymbol{w}^{\boldsymbol{T}}[\boldsymbol{n}]\boldsymbol{v}[n]. \tag{5-52}$$

Accordingly, the weight update equation becomes:

$$\boldsymbol{w}[n+1] = \boldsymbol{w}[n] + \mu\, \mathcal{E}\{e[n]\boldsymbol{v}[n]\}. \tag{5-53}$$

In practice, the expected value $\mathcal{E}\{e[n]\boldsymbol{v}[n]\}$ is not known and needs to be estimated. It can be simply replaced by taking its instantaneous estimate at time n, i.e., $\mathcal{E}\{e[n]\boldsymbol{v}[n]\} = e[n]\boldsymbol{v}[n]$. Thus,

$$\boldsymbol{w}[n+1] = \boldsymbol{w}[n] + \mu\, e[n]\boldsymbol{v}[n]. \tag{5-54}$$

Typically, the LMS algorithm is initialized by setting all weights equal to zero, i.e., $\boldsymbol{w}[0] = \boldsymbol{0}$. The block diagram in Figure 5-11 illustrates the LMS-based artifact cancellation technique.

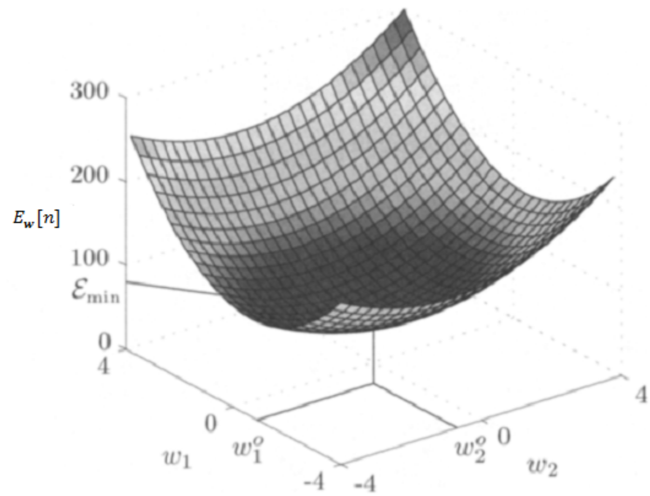

Figure 5-10: The quadratic error surface, $E_w\,[n]$ plotted as a function of weight vector w_1, w_2 [2].

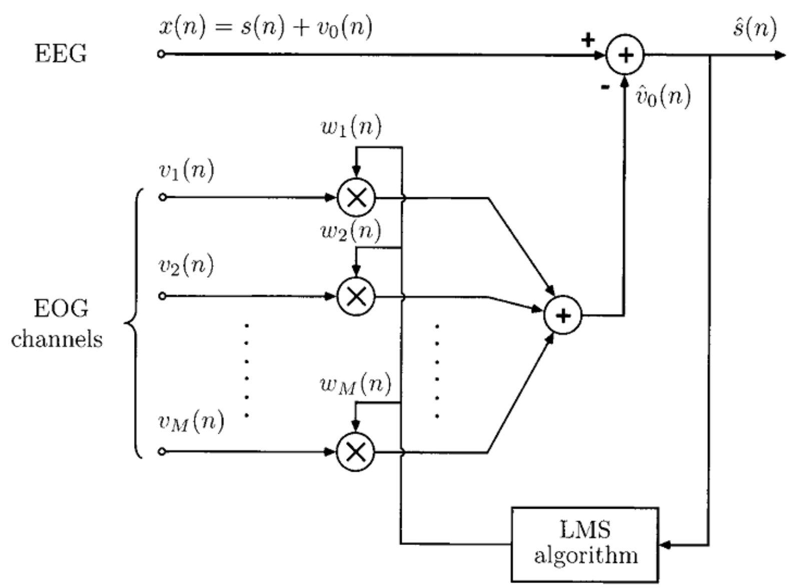

Figure 5-11: EOG artifact cancellation using a linear combination of EOG signals with adaptively updated weights [2].

A generalized version of these algorithms is obtained by replacing the linear weights (i.e., w_i) by LTI systems with impulse responses, h_i (see Figure 5-12). Error minimization in this method is beyond the scope of this course, therefore, it won't be touched in this lecture notes. Independent

Component Analysis (ICA) is another method which is widely used for EOG artifact cancellation in EEG. Interested readers are referred to this paper for more details.

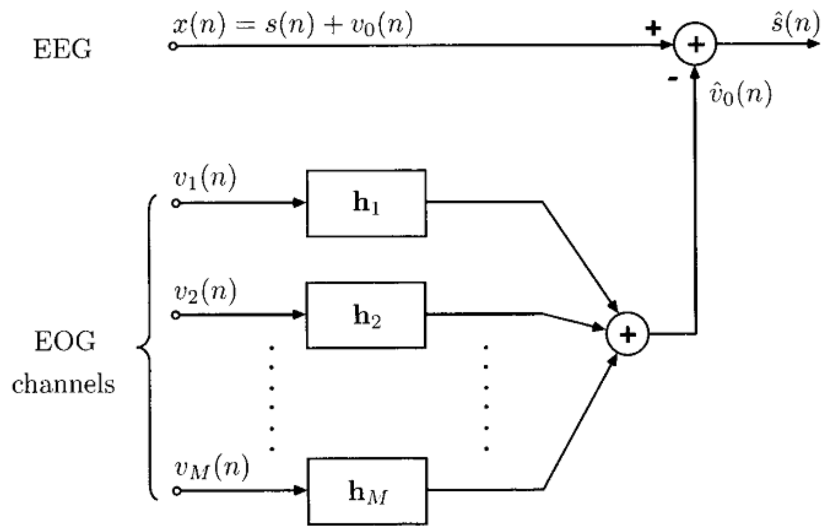

Figure 5-12: Cancellation of eye movement artifacts using an estimate based on linear FIR filtering of M different EOG channels [2].